bioresources.com

The Detection of Structure in Wood by X-Ray CT Imaging Technique

Zhedong Ge,[a,*] Longxian Chen,[a] Rui Luo,[a] Yanwei Wang,[b] and Yucheng Zhou [a]

Medical computed tomography (CT) has been used in forestry science and the wood industry to explore the internal structures of trees in a non-destructive way. The wood material has great diversity in structure, density, and size. The software system for medical CT is not applicable to analyze and process sectional images of wood. In order to solve this problem, a CT imaging system, based on the principle of X-ray fan-beam scanning, was constructed for this study. The computer tomography technique was applied in the non-destructive testing of wood. Four kinds of representative specimens—laminated wood, multi knot logs, large diameter logs, and small diameter logs—were selected as scanned objects. The sinusoidal images and sectional images were reconstructed with scanning data. The results showed that the accuracy of CT images is determined by the information in the sinusoidal images, from which the shapes and locations of cracks and knots can be identified. The internal properties of wood in some tomography, such as the size, number, and location of cracks and knots, the number of tree rings, and the growth law of early wood and late wood can be visually observed. Finally, the feasibility and validity of the CT imaging system was tested as a non-destructive method for verifying the internal structures of wood.

*Contact information: a: School of Information and Electrical Engineering, Shandong Jianzhu University, Jinan, 250101, China; b: Research Institute of Wood Industry, Chinese Academy of Forestry, Beijing, 100091, China; *Corresponding author: gezhedong@163.com*

INTRODUCTION

Wood, as a biomass material, has many advantages, such as beautiful texture, high strength, high quality, and no environmental pollution. Wood is an indispensable material for furniture, decoration, and buildings because of its reproducibility and workability. Thus, wood plays an important role in human life. Studying wood structure characteristics and defects is good for property analysis, scientific processing, high-efficiency utilization, and dividing rank on wood according to the different features (Fredriksson 2015). The quality of wood surfaces may be observed easily, but the structural features and growth defects in wood are difficult to obtain by its appearance alone. The conventional method of observing the internal structure of wood is cutting down the tree or using non-destructive testing technology such as stress wave, ultrasonic wave, and X-ray computed tomography (CT). CT is an advanced non-destructive testing technology that has been widely used in medicine, industry, and agriculture (Hong *et al*. 2014; Zhang *et al* 2014; Ma *et*. 2017; Rais *et al*. 2017). In the 1990s, medical CT equipment was applied to explore the internal structural characteristics of wood and building materials (Jacobs *et al*. 1995; Livingston 1999). Some experimental tests were conducted on Norway spruce, and the size of the knots and the boundaries of the dead

knots were identified through the sectional image (Oja 1999). Wei *et al*. (2008) proposed an algorithm that detects internal structural characteristics of wood, such as knots, bark, sapwood, and heartwood of sugar maple. However, CT is a medical instrument mainly used for human disease detection. Due to the diversity and complexity of wood, the analysis and treatment of the software system for medical CT are not directly applicable to reconstructed images of wood. In order to reduce the damage to people, the voltage of the X-ray source of medical CT is usually less than 140 kV, so the X-ray cannot penetrate wood when the diameter and density of wood are greater than the human body. Fixed and immovable objects, such as trees and columns of buildings, cannot be scanned by medical CT. Therefore, medical CT is not suitable for the research and application in the field of wood science. In order to expand the application of CT technology in the field of non-destructive wood testing, a CT tomography test platform has been developed to collect projection data of several kinds of wood, as shown in Fig. 1 (Ge *et al*. 2016). The projection data are used to reconstruct sectional images, based on which internal structural properties of wood can be observed and analyzed. This technique provides a new detection method for the non-destructive testing of wood and standing timber.

Fig. 1. A nondestructive testing system for living trees

EXPERIMENTAL

Principles of X-ray Scanning Technology

Wood is a heterogeneous material with characteristics of biomass. Its structure is related to the tree species and the growth environment (Muzamal *et al*. 2016). When an X-ray passes through the wood at various scanning angles, the energy absorbed by the wood must be different. Thus, a two-dimensional distribution matrix of the attenuation system value on the scanning section can be obtained by measuring the attenuation coefficients of X-rays in different paths within the wood. The elements of the matrix consist of the attenuation coefficients. A sectional image can be reconstructed out of the scanned data (Longuetaud *et al*. 2012; De e*t al*. 2016).
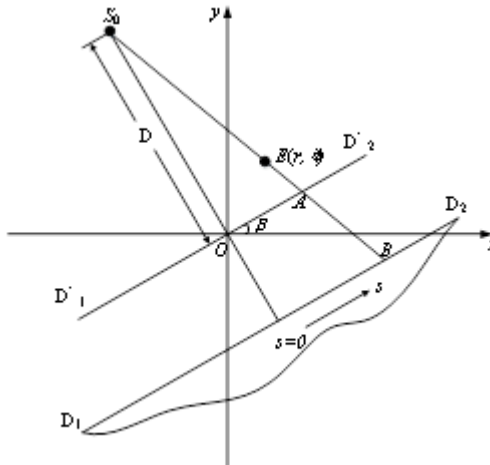
Fig. 2. The parameter relation of equidistance fan beams

The image reconstruction principle of the CT system was analyzed to verify that there was a functional relation between the projection address of a certain detecting point in the scanning fault and the rotation angle. The trajectory of projection addresses was a sinusoidal curve associated with the rotation angles during the scanning process (Zhuang 1992). As shown in Fig. 2, the X-ray source S_0 launches a fan-beam along a path AB through the E point in the detected object. The attenuated ray is received by the X-ray detector D_1D_2. By measuring the energy of the ray passing through a certain detecting point at different angles and then by using the filtered back projection algorithm, the sectional image of the detected object can be reconstructed. Two sets of projection data are collected. I_0 represents the intensity of the ray of the source and I denotes the intensity of the ray after passing through the object, which are given in Eqs. 1 and 2,

$$I_0 = \begin{bmatrix} I_{0(1,1)} & \cdots & I_{0(1,1280)} \\ \vdots & I_{0(\beta,s)} & \vdots \\ I_{0(360,1)} & \cdots & I_{0(360,1280)} \end{bmatrix} \tag{1}$$

$$I = \begin{bmatrix} I_{(1,1)} & \cdots & I_{(1,1280)} \\ \vdots & I_{(\beta,s)} & \vdots \\ I_{(360,1)} & \cdots & I_{(360,1280)} \end{bmatrix} \tag{2}$$

where $I_{0(\beta,s)}$ is the intensity of the ray received by the s-th probe point at the scanning angle β and $I_{(\beta,s)}$ denotes the intensity of the ray received by the s-th probe point at the scanning angle β after passing through the detected object.

Based on the Cartesian coordinate system, the coordinate of any point E in the scanning section is represented by (x, y), which can be regarded as a very small rectangular region. The attenuation coefficient of this region is defined as $f(x, y)$. Thus, the ray projection through (x, y) can also be represented by $P(x, y)$ (Eq. 3; You and Zeng 2007; Krähenbühl *et al*. 2014),

$$P(x,y) = \iint f(x,y)dxdy = \ln\left(\frac{I_0}{I}\right) \tag{3}$$

where I_0/I represents the division element by element.

A polar coordinate system r-φ can also be used, denoted by (r, φ). When the angle is β, the ray projection value $P(x, y)$ is expressed as $g_\beta(s)$. Assume that the transfer function of the filter is $h(s)$. $g_\beta(s) * h(s)$, which represents the convolution between $h(s)$ and the projection value $g_\beta(s)$ received by the X-ray detector at every angle. According to the filtered back projection algorithm, the back projection values $a(r, \varphi)$ of each angle at point E is obtained by integrating $g_\beta(s) * h(s)$ along β. Then, it is converted to grayscale with a range of 0 to 255. Finally, the new pixel values are generated to reconstruct a sectional image, as shown in Eq. 4.

$$a(r, \varphi) = \int_0^{2\pi} g_\beta(s) * h(s) d_\beta \qquad (4)$$

Wood Specimens

The wood structure is complex, and the shape is changeable. As shown in Table 1, four specimens with different structural characteristics were randomly selected and scanned for the image reconstruction and defect detection. The specimens included laminated wood, a log with multiple knots, a large diameter log, and a small diameter log. The laminated wood was composed of four 20 mm thick chord cutting plates, and its structure was similar to wood used for furniture. The log with multiple knots had several knots and a crack along the radial direction. The large diameter log had cracks along the radial direction with a good wood surface and no other defects. The small diameter wood had several cracks with different widths and lengths and knots extending outside of the wood. The experimental materials are shown in Table 1.

Table 1. Experimental Materials

Projects	1	2	3	4
Name	Laminated Wood	Multi Knots Log	Large diameter Log	Small diameter Log
Producing area	Su' qian City of Jiangsu Province	Kai' hua City of Zhejiang Province	Lin' an City of Zhejiang Province	Lin' an City of Zhejiang Province
Diameter / mm	-	133	205	95
Density / (g/cm^3)	0.32	0.28	0.37	0.37
Specimens				

Experimental Equipment

As shown in Fig. 3, a wood CT imaging system was constructed in the laboratory. It was composed of an X-ray emitter, an X-ray detector, a platform with lifting and

rotating, and a computer (Ge *et al*. 2016). The computer was used for reconstructing, processing, and analyzing images. The output power of the X-ray emitter was 500 W. Its maximum ray angle was 80º, and its focal spot size was 0.05 mm. The working voltage and current were adjusted continuously between 10 to 160 kV and 0 to 3.12 mA, respectively. The detector contained ten pieces of XDAS-DH analog data acquisition boards, two pieces of XDAS-SP digital signal processing boards, and one piece of XDAS-USB data output module. Its effective detection length was 512 mm with a linear array of 1280 pixels, with each pixel size being 0.4 mm × 0.4 mm. The rotational speed and height of the platform were driven by two stepper motors. The range of lifting was from -200 mm to +200 mm. The maximum detection diameter was 27 mm, and the maximum detection length was 400 mm.

Fig. 3. A nondestructive testing system for wood

Methods

A specimen was fixed at the rotating center of the platform between the emitter and the detector. It was 566 mm away from the emitter and 391 mm away from the detector. The working voltage and current of the ray source were set to 120 kV and 0.7 mA, respectively, and the integral time of the detector was set to 5000 s. For this study, the detector was turned on, the platform was rotated, and the emitter was started, in sequence. The rotational speed of the platform was 1.5º/s, and the scanning cycle was 360º. The X-ray from the collimator went through the specimen and irradiated on the probe points arranged linearly.

The attenuated X-ray was received and converted into digital signals by the detector. The projection values were transmitted to the computer and saved as the data file. The data contained some irregular values (for example, values that are much bigger or smaller than those in their neighborhood) or unnecessary values (for instance, values for the angles beyond 0 to 360º), which were removed first. For image reconstruction, a filter was used to process the data and extract the corresponding projection data according to the projected coordinate value in advance.

Self-developed software was used to process and analyze the sectional image and to output the image on the computer screen to determine the internal defects. This system can shorten the image reconstruction time of CT system to less than 1s and the image resolution can reach 0.052 mm^2.

RESULTS AND DISCUSSION

The Sectional Image of a Laminated Wood

Laminated wood (also called laminated timber) is an important building material and decoration material. A laminated wood from Su' qian City, Jiangsu Province, China was selected as the test specimen. Its size was 80 mm $\times$ 160 mm $\times$ 500 mm, and its density was 0.32 g/cm^3. It was made of four layers of solid wood sheets of 20 mm in different texture directions.

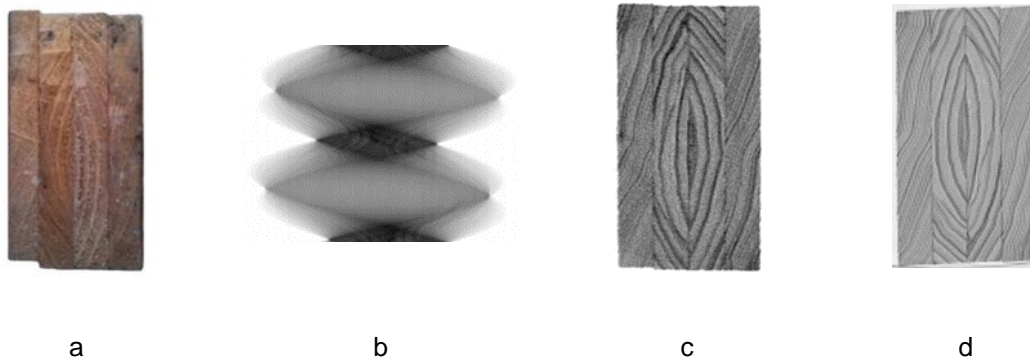a   b   c   d

Fig. 4. The reconstructed results of the laminated wood; (a) the photograph of the laminated wood; (b) sinusoidal image of the laminated wood; (c) sectional image of the laminated wood with nondestructive testing system; (d) sectional image of the laminated wood with medical CT

Based on the image reconstruction algorithm for fan-beam CT, the projection trajectory of each pixel on the laminated wood section at different angles was obtained. Therefore, a sinusoidal image was constructed by using many sine curves (Fig. 4). Because the laminated wood was a rectangular specimen, the sinusoidal image was composed of several diamonds with different gray values. The laminated wood with a smaller rotation angle was in a vertical direction for a short time. The X-ray passed through the laminated wood over a long path and its energy decayed greatly. Because the detector received less energy, small diamond shapes in the sinusoidal image were composed of some light pixels. The laminated wood with a bigger rotation angle was in a horizontal direction for a long time. The X-ray passed through the laminated wood over a short path and its energy decayed slowly. Because the detector received more energy, big diamond shapes in the sinusoidal image were composed of some dark pixels. The sine curves were clear, natural, and smooth, which showed that there was no abnormal structure inside the specimen. The sectional image showed no artifacts. The specimen was composed of four layers of solid wood sheets together. The bonding lines were obvious, and the featured textures of each plate were clear, natural, and orderly. Two pieces of plates with wide tree rings in the middle of laminated wood were glued together in opposite directions of textures. The other two pieces of plates with narrow tree rings in the left and right sides were glued in the same direction of textures. By comparing the photograph and reconstructed sectional image, the two images show the same section structure of the laminated wood.

Sectional Images of the Log with Multiple Knots

Knots are included in the main part of a trunk or some branches of the xylem. A knot is a normal physiological phenomenon in trees. However, it is an enormous defect in terms of the use of the wood, and it has a great influence on the mechanical properties and texture. A log with multiple knots and a diameter and density of 133 mm and 0.28 g/cm³, respectively, was taken from the Kai' hua City of Zhejiang Province, China. A transverse section with multiple knots and a crack in the vertical extension is shown in Fig. 3.
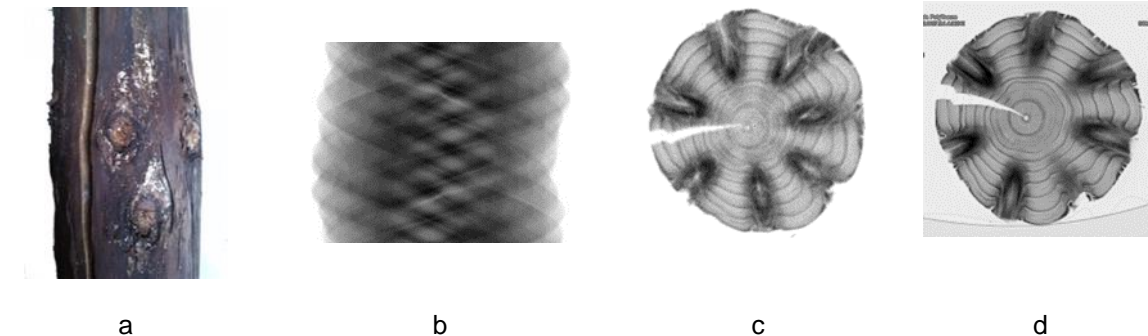

a   b   c   d

Fig. 5. The reconstructed results of the log with multiple knots; (a) the photograph of the log; (b) the sinusoidal image of the log; (c) the sectional image of the log with nondestructive testing system; (d) sectional image of the log with medical CT

Because seven black sinusoidal curves are clearly visible from the sinusoidal image, there may be seven abnormal structures in the wood. Compared with the surrounding area, the density of the abnormal structure was larger. There was one lighter sine curve in the sinusoidal image, which may have been a crack. There were many patterns in the sinusoidal image, each of which formed a complete sine curve. The sectional image of the wood shows that there were some annular artifacts in the central region. The internal rings, cracks, and knots were visible as well. The boundaries of the outer rings were obvious, but the inner rings were not clear because of the interference of the annular artifacts. The crack was larger at the opening and became steadily smaller towards the pith of the wood. In deep contrast to other structures, there were seven different sizes of knots inside of the wood, evenly distributed around the heartwood with darker color.

The Sectional Image of a Large Diameter Log

In this experiment, logs with diameter greater than 200 mm were considered as large diameter logs. A specimen with the diameter of 205 mm and the density of 0.37 g/cm³ was taken from Lin' an City, Zhejiang Province, China. Apart from the cracks, the wood had no other defects, and its surface was smooth.

The sinusoidal image of the large diameter log is shown in Fig. 6. A white sine curve was observed clearly. Actually, the sine curve is the projection trajectory of two cracks. The cracks are very close, which makes it difficult to distinguish from the sinusoidal image. In the sectional image of the wood, the heartwood was lighter in color, and the tree rings were distributed evenly. The sapwood was dark in color, and the tree rings were too close to distinguish from the wood. There were two cracks with smooth

edges. The wide crack extended to the heartwood and was combined with the narrow crack extending to the pith. The sectional image shows that each structure of the wood is very clear, and it is difficult for the naked eye to observe ring artifacts. Therefore, the transverse section of the wood was completely observed from the sectional image.
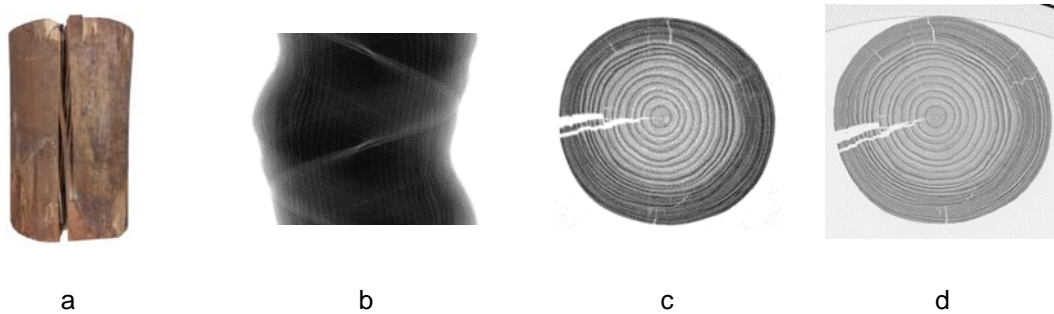

a   b   c   d

Fig. 6. The reconstructed results of the large diameter log; (a) the photograph of the large diameter log; (b) the sinusoidal image of the large diameter log; (c) the sectional image of the large diameter log with nondestructive testing system; (d) sectional image of the large diameter log with medical CT

The medical CT is a device for human detection and the reconstructed image is processed. This process will inevitably lose a part of the information, which should not be supposed to appear. From the results of the detection of wood by the medical CT, the internal structure of wood is very smooth, because the filter function is used in the reconstruction process and many factors are eliminated. But the content that has been eliminated still has some value for wood science research and needs to be preserved.

The Sectional Image of a Small Diameter Log

In the experiment, logs with diameter less than 100 mm were considered as small diameter logs. A specimen with the diameter of 95 mm and the density of 0.37 g/cm^3 was collected from Lin' an City, Zhejiang Province, China. There were two kinds of defects, such as cracks and knots, in this wood. The width and length of cracks were different from each other, and the knots grew from inside to outside of the wood.
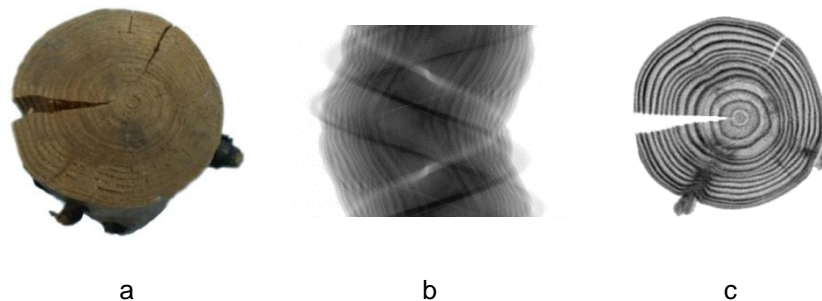

a   b   c

Fig. 7. The reconstructed results of the small diameter log; (a) the photograph of the small diameter log; (b) the sinusoidal image of the small diameter log; (c) the sectional image of the small diameter log

Three sine curves were observed in the sinusoidal image of the small diameter log. One white sine curve was the projection trajectory of a large crack, and the other two

black sine curves were projection trajectories of two knots. From the sectional image, a large crack extended to the center of the wood, and a small crack was in the upper-right of the image. The boundaries of early wood and late wood, which formed thirteen irregular tree rings, were clearly observed. There were few noise pixels in the sectional image, the edge of which was clear with smoothly transitional colors. In the photograph, there were three cracks. One was big, located on the left, and the other two were small and located on the top. Two knots grew from the inside to the outside. In the sectional image, there were two cracks and a knot. The smallest crack at the top of the wood did not extend to the base of the wood. Two knots were not growing on the same layer, and the scanning section passed though one of the knots. Thus, only one small crack was found on the top except for a large crack, and only one knot was found on the bottom left. The other knot on the bottom right was vague.

Tomography Images of the Log

The wood CT imaging system is mainly used to identify and detect the internal structure of wood. In order to research growth laws of cracks, knots, and tree rings in different scanning sections, a small diameter log was taken as the scanned object. The projection data were obtained for three sections with one section cutting the knot, one above, and one below. The distance of adjacent sections was 5 mm. The reconstruction results are shown in Fig. 8.
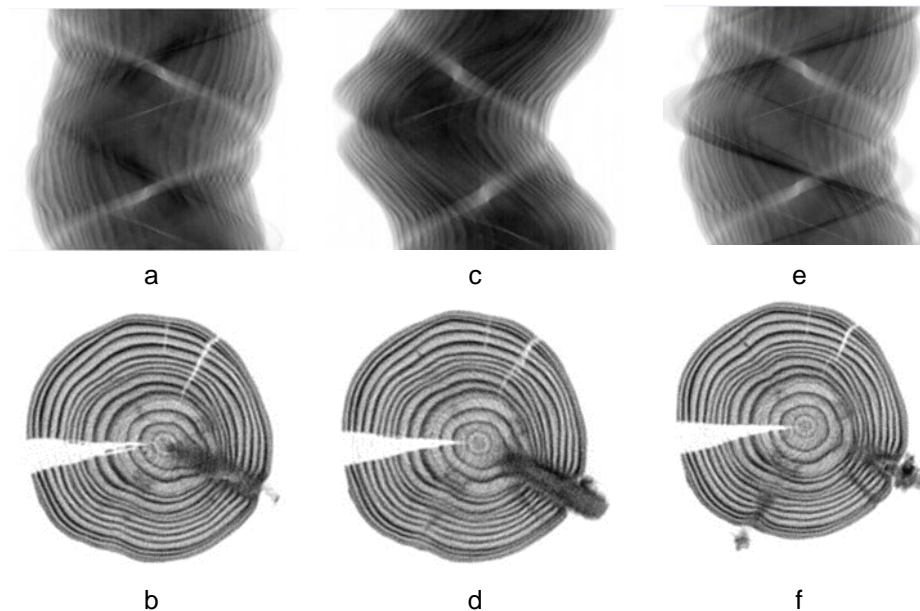

a   c   e

b   d   f

Fig. 8. The reconstructed results of different transverse sections; (a) the sinusoidal image above the knot; (b) the sectional image above the knot; (c) the sinusoidal image in the middle of knot; (d) the sectional image in the middle of knot; (e) the sinusoidal image under the knot; (f) the sectional image under the knot

There is a common characteristic, such as a thick white sine curve, in the three sinusoidal images. The wave crest is on the left and the wave trough is on the right. Compared with the three sectional images, the thick white sine curve is the projection trajectory of the big crack on the left and the thin white sine curve is the projection trajectory of the small crack on the upper-right, which are obtained when the wood

rotates one complete cycle. In addition, a thin white sine curve was found clearly away from the thick white sine curve and the phase angle between them is about 110º, which can be verified by observing the three sectional images. The three sectional images show that the angle between the small crack and wide crack is 110º. Therefore, much information about the sectional image is contained in the sinusoidal image.

The sinusoidal and sectional images of a scanning section above the knot are shown in Figs. 8a and b. Comparing Figs. 8a and b, the dark sine curve is the projection trajectory of the knot on the bottom right, and the thick and thin light sine curves are projection trajectories of the big and small cracks, respectively. In Fig. 8a, the phase angle between the dark and light sine curves is about 170º; thus, the angle between the knot and the big crack is 170º. This conclusion was confirmed by observing the locations of the knot and the big crack in Fig. 8b. In addition, it can be seen from Fig. 8a that the phase angle between the thin light and dark sine curves is 90º, as a result, the angle between the small crack and knot is 90º, which can be verified by looking at the locations of the small crack and knot in Fig. 8b. The same conclusions can be drawn from Figs. 8e and f, which display the sinusoidal and sectional images of a scanning section below the knot. It can be observed from Fig. 8b that the big knot on the bottom right starts from the pith and extends to the bark. The image of the same knot moves outside so that 2/3 of the knot is embedded in the xylem and 1/3 of the knot extends to the outside of the bark in Fig. 8d. In Fig. 8f, a knot is found on the bottom left, which is separated from the transverse section image of the wood. It has been demonstrated that the knot is growing upward. Three sectional images (Figs. 8b, d, and f) are 3 sections respectively, one above the knot, one cutting the knot, and one below the knot. There are some common characteristics in the above images, such as a big crack extending to the pith of wood on the left and two smaller cracks on the top. The position of section is lower and the distance of the crack extending into the wood internally is shorter. Compared with the characteristics of the knot on the bottom right, the growth law is found. The knot extends from the interior of the wood to the exterior and then grows upward. The section of the knot on the bottom left is only shown in Fig. 8f because the knot is growing on the lower section. If the scanning is carried out for the bottom of the wood structure, the sectional image of the knot on the bottom left can be obtained.

CONCLUSIONS

1. Cracks, knots, and rings are important macroscopic structures and have important effects on the properties and textures of wood. In this paper, a laminated wood, a log with multiple knots, a large diameter log, and a small diameter log having different macroscopic structures including tree rings, cracks, and knots were selected randomly as samples for scanning. The reconstruction shows that a large amount of information is saved in sinusoidal images, and it can affect the accuracy of sectional images. Some macroscopic structures of wood on a section can be observed visually in the sectional image, such as the size, number, angle, and location of the crack, the number of knots and tree rings, and the growth law of the early wood and late wood.

2. CT technology, as an advanced nondestructive detection method, is of great value for research on the physiological structure of wood. At present, it is mainly used for studying internal structure and finding the location of defects in wood. In this paper, a

CT imaging system can be used to construct the high-quality sectional image of wood, but the software function of the system is not very powerful. For example, cracks, knots, tree rings, heartwood, and sapwood still need to be identified by experienced researchers. The future direction of research is image segmentation, image component modeling, image analysis, and reasoning. Based on sinusoidal images and sectional images, the information of macroscopic structures in wood, such as the number of knots, the angles of cracks, the diameter of the tree, the boundary of heartwood and sapwood, should be obtained automatically for image segmentation and feature extraction. Therefore, there are some limitations in the image processing and analysis function of the CT software system, and the algorithm of image segmentation and feature extraction needs to be optimized. The wood CT imaging system and the powerful image analysis software will be more useful to scientific research on wood.

ACKNOWLEDGMENTS

REFERENCES CITED

De, M. T., Vannoppen, A., Beeckman, H., Van, A. J., and Van, d. B. J. (2016). "A field-to-desktop toolchain for x-ray ct densitometry enables tree ring analysis," *Ann Bot* 117(7), 1187-1196. DOI: 10.1093/aob/mcw063

Fredriksson, M. (2015). "Optimizing sawing of boards for furniture production using CT log scanning," *J. Wood Sci.* 61(5), 474-480. DOI: 10.1007/s10086-015-1500-0

Ge, Z. D., Hou, X. P., Li, Z. F., and Zhou, Y. C. (2016). "Application of computed tomography (CT) in nondestructive testing of wood," *China Wood Industry* 30(3), 49-52. DOI: 10.3969/j.issn.1001-8654.2016.03.012

Ge, Z. D., Hou, X. P., Lu, S. Y., Qi, Y. H., Zhang, G. L., and Zhou, Y. C. (2016). "Wood CT detection system based on fast algorithm of inverse projection coordinate," *Transactions of the Chinese Society for Agricultural Machinery* 47(3), 335-341. DOI: 10.6041/j.issn.1000-1298.2016.03.047

Hong, G. Z., Mao, C., and Wang, X. W. (2014). "Research on meat thickness measurement based on laser double-triangulation method," *Transactions of the Chinese Society for Agricultural Machinery* 45(9), 223-229. DOI:10.6041/j.issn.1000-1298.2014.09.036

Jacobs, P., Sevens, E., and Kunnen, M. (1995). "Principles of computerized X-ray tomography and applications to building materials," *The Science of the Total Environment* 167(1-3), 161-170. DOI: 10.1016/0048-9697(95)04577-N

Krähenbühl, A., Kerautret, B., Debled-Rennesson, I., Mothe, F., and Longuetaud, F. (2014). "Knot segmentation in 3D CT images of wet wood," *Comm. Com. Inf. Sc.* 47(12), 3852-3869. DOI: 10.1016/j.patcog.2014.05.015

Livingston, R. A. (1999). "Nondestructive testing of historic structures," *Archives and Museum Informatics* 13(3-4), 249-271. DOI: 10.1023/A:1012416309607

Longuetaud, F., Mothe, F., Kerautret, B., Krähenbühl, A., Hory, L., Leban, J. M., and Debled-Rennesson, I. (2012). "Automatic knot detection and measurements from X-ray CT images of wood: A review and validation of an improved algorithm on softwood samples," *Comput. Electron. Agr.* 85(5), 77-89. DOI: 10.1016/j.compag.2012.03.013

Ma, L., Liu, X. B., Gao. Y., Zhao Y. F., Zhao, X. M., and Zhou, C. W. (2017). "A new method of content based medical image retrieval and its applications to CT imaging sign retrieval," *Journal of Biomedical Informatics* 66(C), 148-158.

Muzamal, M., Bååth, J. A., Olsson, L., and Rasmuson, A. (2016). "Contribution of structural modification to enhanced enzymatic hydrolysis and 3-D structural analysis of steam-exploded wood using X-ray tomography," *BioResources* 11(4), 8509-8521. DOI: 10.15376/biores.11.4.8509-8521

Oja, J. (1999). *X-ray Measurements of Properties of Saw Logs*, Ph.D. Dissertation, Luleå University of Technology, Luleå, Sweden.

Rais, A., Ursella, E., Vicario, E., and Giudiceandrea, F. (2017). "The use of the first industrial X-ray CT scanner increases the lumber recovery value: Case study on visually strength-graded Douglas-fir timber," *Annals of Forest Science* 74(2), 28-36. DOI: 10.1007/s13595-017-0630-5

Wei, Q., Leblon, B., Chui, Y. H., and Zhang, S. Y. (2008). "Identification of selected log characteristics from computed tomography images of sugar maple logs using maximum likelihood classifier and textural analysis," *Holzforschung* 62(4), 441-47. DOI: 10.1515/HF.2008.077

You, J. S., and Zeng, G. L. (2007). "Hilbert transform based FBP algorithm for fan-beam CT full and partial scans," *IEEE T. Med. Imaging* 26(2), 190-199. DOI: 10.1109/TMI.2006.889705

Zhang, J. P., Zhu, J. X., and Sun, T. (2014). "Detection of apples' internal quality using CT imaging technology and Fourier transform," *Transactions of the Chinese Society for Agricultural Machinery* 45(3), 197-204. DOI:10.6041/j.issn.1000-1298.2014.05.031

Zhuang, T. G. (1992). *The Principle and Algorithm of CT*, Profile of Shanghai Jiao Tong University Press, 24-29.